

PRODUCTION PROCESS RETENTION USING A FLOW ANALYSIS IN THE MANUFACTURING BUSINESS

KENJI SHIRAI¹ AND YOSHINORI AMANO²

¹Faculty of Information Culture
Niigata University of International and Information Studies
3-1-1, Mizukino, Nishi-ku, Niigata 950-2292, Japan
shirai@nuis.ac.jp

²Kyohnan Elecs Co., LTD.
8-48-2, Fukakusanishiura-cho, Fushimi-ku, Kyoto 612-0029, Japan
y_amano@kyohnan-elecs.co.jp

Received March 2017; revised July 2017

ABSTRACT. *In manufacturing processes, the production process may be forced to stop when, for example, there are uncertain production plans, delays in logistics, cancelations of orders, etc. In this paper, we mathematically analyze the types of situations that occur before and after such stops in production. We introduce the concept of a shock wave to denote the effects these before and after occurrences have on the production process. More specifically, we define the shock wave here by the propagation of production density flows in Burgers equation. We propose a propagation flow equation for a production density; here, the propagation of a shock wave is equal to the change in production density after production transitions from a stopped state back to a start state. In other words, the propagation of shock waves is a phenomenon of queuing time constraints due to retention.*

Keywords: Shock wave, Burgers equation, Production density, Process retention, Production process

1. Introduction. In a previous study, the problem of reducing construction work and inventory in the steel industry was reported [1]. Specifically, we investigated the relationship between variations in the rate of construction and delivery rate was interesting.

Moreover, several studies have reported approaches that lead to shorter lead times [2, 3]. From order products, lead time occurs on the work required preparation of the members for manufacturing.

Many aspects can potentially affect lead time. For example, from order products, the lead time from the start of development to the completion of a product is called the time-to-finish time, such as the work required preparation of the members for production equipments.

Moreover, with respect to reducing customer lead times, the problem of reducing the production lead time was reported [4].

On the other hand, fluctuations in the supply chain and market demand and the changes in the production volume of suppliers are propagated to other suppliers, and their effects are amplified. Therefore, because amounts of stock are large, an increase or decrease of the suppliers' stock is modeled using differential equation. This differential equation is said as Billwhip model, representing a stock congestion [6, 7]. These studies are very interesting contents.

The theory of constraints (“TOC”) describes the importance of avoiding bottlenecks in production processes [8]. When using manufacturing equipment, delays in one production

step are propagated to the next. Hence, the use of manufacturing equipment may lead to delays. “TOC” gives important suggestions for increasing efficiency of production projects. There is no research that mathematically models propagation of production density.

Many currently implemented production systems are mechanized and highly integrated with information technologies, which creates systems where human intervention is unnecessary. In certain aspects of the production system, there is a high volume of build-to-order manufacturing that requires human intervention in the production process [9, 10]. In small- and medium-sized enterprises, human intervention constitutes a significant part of the production process, and revenue can sometimes be greatly affected by human behavior. Therefore, with respect to human intervention with outside companies, a deep analysis of the production process and human collaboration is necessary to understand the potential negative effects of human intervention [9, 10]. Naturally, the effect of human behavior is not just a problem with small- and medium-sized companies; it must be regarded as one of the major problems that may occur when humans directly intervene in the production process [11, 12, 13].

In general, the potential uncertainties should be considered before proceeding with a system that combines human intervention (Internal force) with outside companies (External force) in the production system [14, 15]. With respect to two elements in a production system, a total system is formed by connecting the two elements. In this case, a system with certain uncertainties will be formed when connecting “human intervention” and “outside companies” in a production system. In general, an important concept in the production system is to develop the best system that results in efficient production. However, in most analyses of the production process, researchers have not taken advantage of the noise inherent in the system. Such noise may have a unique usefulness in the system.

Thus, we have been researching mathematical modeling and system evaluations from a physical point of view to develop “mathematical production engineering” in order to develop a mathematical system for describing production processes. In a previous study of stochastic modeling, we considered the internal force and external force as parameters in a production system. The correlation of lead time vs. throughput is important for implementing the overall synchronization as a strategy. We had reported a production system with an intervention of workers in the prior study [14, 15]. In case of a production flow system with human intervention, we need to fulfill an empirical analysis of worker-specific production ability. Thus, to achieve optimal general production systems, knowledge of the importance of biological fluctuations in the system is important.

In our previous study, we determined and showed that an on-off intermittency exists in rate-of-return and lead time deviations of production processes. In physics, an on-off intermittency is present in power-law distributions, phase transitions, and self-similar phenomena. In the production process described in the present study, we observed on-off intermittency on lead time data with respect to time series datasets [16]. In our previous work, we reported that by creating a state in which the production density of each process corresponds to their physical propagation, the manufacturing process is most appropriately described using a diffusion equation [9]. In other words, if the potential of the production field (i.e., stochastic field) is minimized, the equation is defined by production density function $S_i(x, t)$ and the constraint is described using an advective diffusion equation to determine transportation speed ρ [9, 17].

Based on results from our previous study, we can observe and link the on-off intermittence in time with fluctuations that we previously reported in 2014 [16]. More specifically, we reported a stochastic resonance phenomenon in production processes, clarifying that

intervention by outside companies and workers (i.e., an internal force) was treated as input noise (i.e., stochastic element) to successive processes in the production system [18]. Further, we reported that we analyzed the cause of fluctuations in the lead time of production processes by applying a phase-field model, a new approach by which we clarified that the occurrence factors were attributed to state variables corresponding to an internal process. Factors of such fluctuations included the uncertainty of logistics, uncertainty of production planning, and stochastic characteristics of the order and start time series [20].

In this paper, we note that the fluctuation in lead time is caused by the propagation of the fluctuation of state variables constrained by Burgers' equation from fluid dynamics. We derive Burgers' equation by recognizing the graph of the start time series (i.e., order time-series) of the lead time period in production processes. Here, we observe in production processes a phenomenon similar to that of turbulent flow fields in fluid dynamics [21]. More specifically, we utilize Burgers' equation to analyze the shock wave propagation of production processes, where we define our shock wave propagation term further below. The factors that cause these fluctuations include the following:

- Uncertainty of logistics
- Uncertainty of production planning
- Stochastic characteristics of the order and start time series

In practice, production processes may suddenly stop due to, for example, uncertain production plans, delays in logistics, and cancelations of orders. In this paper, we, therefore, mathematically analyze the phenomena that occur before and after such interruptions in production. Here, we modeled the propagation of production density using heat conduction equations, using Burgers' equations as a base. We define the shock wave as the propagation of production density flows using Burgers' equations. Further, we propose the propagation flow equation for production density. The propagation of a shock wave is equal to the change in production density after the production process transitions from a stopped state to a start state, i.e., the propagation of shock waves is a phenomenon of queuing time constraints due to retention. From our research results, we note that the diffusion coefficient affects the fluctuation in turbulent spots just as in fluid mechanics. When the configuration parameters of the diffusion coefficient are considered as trend coefficients and volatility, a production process can be modeled as a synchronous process, such as laminar flow in fluid dynamics, by reducing the volatility of the production processes. We also implemented a dynamic simulation to evaluate and confirm the effectiveness of both synchronous and asynchronous processes. To the best of our knowledge, ours is the first study focusing specifically on fluctuations in production processes.

2. Production Retention Analysis.

2.1. Propagation of production density. Figure 1 shows that connection between processes can be treated as diffusive propagation of products [9]. In Figure 1, $C(t, x)$ represents the throughput [9]. In Figure 2, when the advection speed changes, Figure 2(a) shows that the A part moves quickly to the right, and the distance between AB is shortened gradually because the B part moves slowly. Figure 2(b) shows that the A part catches up with the B part and overtakes it after a certain time has elapsed, following which the wave collapses. Figure 2(c) shows that the dissipation area suppresses processes like the wave until a limited gradient forms when the spatial gradient becomes sharp.

Assumption 2.1. *A production flow depends on a production density.*

This assumption is the premise of our previous reports [9, 19].

Definition 2.1.

- $S(t, x)$ denotes a production density.
- $C(t, x)$ denotes a throughput.
- $J(t, x)$ denotes a production flow.

$$J(t, a) - J(t, b) = \frac{d}{dt} \int_a^b S(t, x) dx \tag{1}$$

In Equation (1), $J(t, a) - J(t, b)$ denotes a production flow displacement, and the right hand in Equation (1) denotes as follows.

$$N(t) = \int_a^b S(t, x) dx \tag{2}$$

where $N(T)$ denotes the number of production.

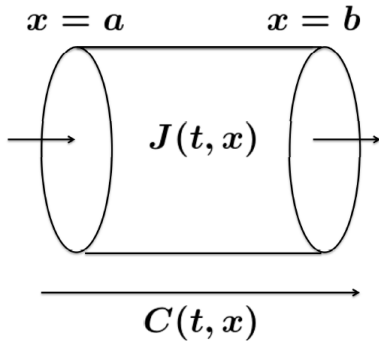


FIGURE 1. Production flow processes

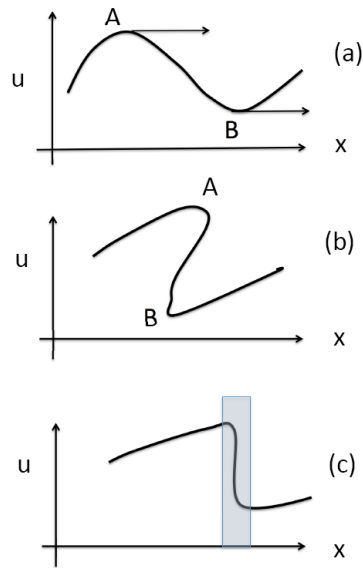


FIGURE 2. Bottleneck phenomenon similar as waves

A production conservation law is established in this production process.

$$\frac{\partial S}{\partial t} + \frac{\partial J}{\partial x} = 0 \tag{3}$$

Then, Equation (1) is rewritten as follows:

$$[J(t, x) - J(t, x + dx)]dt = [S(t + dt, x) - S(t, x)]dx \tag{4}$$

J is proportion to the displacement of $S(t, x)$ as follows:

$$J \sim \frac{\partial S(t, x)}{\partial x} \tag{5}$$

Equation (5) denotes a flow per unit, and the equilibrium equation of production flow is denoted as follows:

$$\frac{\partial J}{\partial x} \cong - \frac{\partial S(t, x)}{\partial x} \tag{6}$$

Assumption 2.2. A throughput $C(t, x)$ depends on a production density $S(t, x)$ and a production flow is described as follows.

$$J(t, x) \equiv C(t, x) \cdot S(t, x) \tag{7}$$

From Equation (6), we obtain as follows.

$$\frac{\partial S(t, x)}{\partial t} + \frac{\partial J}{\partial x} = 0 \tag{8}$$

where the suffix i of S is omitted.

Since throughput depends on production density, we assume as follows:

Assumption 2.3.

$$C(t, x) \cong S(t, x), \quad t \geq 0 \tag{9}$$

where $0 \leq S \leq S_{\max}$, and S_{\max} denotes the maximum of production density.

Furthermore, it is assumed that the throughput decreases as the production density increases.

Assumption 2.4.

$$\frac{dC}{dS} \leq 0, \quad C[S_{\max}] = 0 \tag{10}$$

2.2. Derivation of approximate relational equation in the conservation field of energy. The production density is assumed to be constant at the beginning. Then, we obtain as follows:

$$\frac{\partial S(t, x)}{\partial t} + \frac{dJ}{dS} \frac{\partial S(t, x)}{\partial x} = 0 \tag{11}$$

where $\frac{dJ}{dS}$ represents as follows:

$$v \equiv \frac{dJ}{dS} \tag{12}$$

$$\frac{\partial S(t, x)}{\partial t} + v \frac{\partial S(t, x)}{\partial x} = 0 \tag{13}$$

where we refer to v as the synchronous propagation velocity.

Equation (13) denotes a conservation of energy in the state without input/output.

In this Subsection 2.2, we analyze the case in which production flow stops due to a certain risk. Figure 3 depicts stopped state $x \equiv x_s(t)$ of a production flow. The stopping point, which ceases production due to some sudden set of circumstances during the manufacturing of the given product, is represented by time function $x_s(t)$. Such an interruption results in production cancelation or postponement due to sudden changes in

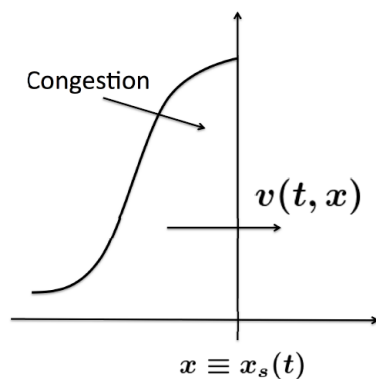


FIGURE 3. Stop in the middle $x \equiv x_s(t)$ of any production flow

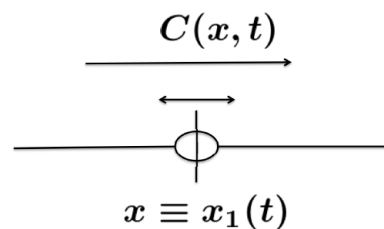


FIGURE 4. Throughput $C(t, x)$

physical conditions, the market, or the circumstances of the customer or customers. In Figure 4, $C(t, x)$ represents the throughput at $x = x_1(t)$ and flows through each process.

In our previous study, we calculated the trend speed by measuring production density at an arbitrary point during production. Note that trend speed here represents the density of product production [9]. Assuming production density is $S(t, x)$ and trend speed is r , we obtain

$$\frac{dr}{dt} = \frac{S(t, a)V(t, a) - S(t, b)V(t, b)}{S^- - S^+} = \frac{S^+V^+ - S^-V^-}{S^- - S^+} \equiv -\frac{S^-V^-}{S^- - S^+} \tag{14}$$

where S^- and S^+ are derived as follows:

$$S^- = \lim_{x \rightarrow r^-(t)} S(t, x) \tag{15}$$

$$S^+ = \lim_{x \rightarrow r^+(t)} S(t, x) \tag{16}$$

where S^- and S^+ denote the limit values of $r^-(t)$ and $r^+(t)$, respectively. In other words, V^+ denotes the speed after the trend and V^- denotes the speed before the trend. Then, we define as follows [9].

Definition 2.2. *Trend speed $V(t)$*

$$V(t) = \frac{-1}{S(t, x)} \frac{d}{dt} \int_a^b S(t, x) dx, \quad t \in [t, t + \delta], \quad x \in [a, b] \tag{17}$$

We define the production flow as follows.

Definition 2.3. *Trend speed $J^-(t, x_s)$ and $J^+(t, x_s)$*

$$J^-(t, x_s) = \lim_{x \rightarrow x_s-0} J(t, x) \tag{18}$$

$$J^+(t, x_s) = \lim_{x \rightarrow x_s+0} J(t, x) \tag{19}$$

Then, the production density is defined according to Equations (18) and (19) as follows.

Definition 2.4. *Trend speed $S^-(x_s, t)$ and $S^+(x_s, t)$*

$$S^-(t, x_s) = \lim_{x \rightarrow x_s-0} S(t, x) \tag{20}$$

$$S^+(t, x_s) = \lim_{x \rightarrow x_s+0} S(t, x) \tag{21}$$

We introduce rate of change of production density [9].

$$x_1(t) = x_s(t) - \delta, \quad x_2(t) = x_s(t) + \delta \tag{22}$$

$$\frac{dV(t)}{dt} = \frac{d}{dt} \int_{x_1(t)}^{x_2(t)} S(t, x) dx \tag{23}$$

$V(t)$ denotes the rate of change of production density in $x \in [x_1(t), x_2(t)]$.

The volume of $J(t, x)$ is derived at $x_1(t)$ as follows:

$$S(t, x) \left\{ C(t, x) - \frac{dx_1(t)}{dt} \right\} = J(t, x_1) - S(t, x_1) \frac{dx_1(t)}{dt} \tag{24}$$

Therefore, we obtain by using Equation (24) as follows:

$$\frac{dV(t)}{dt} = J(t, x_1) - S(t, x_1) \frac{dx_1(t)}{dt} - \left[J(t, x_2) - S(t, x_2) \frac{dx_2(t)}{dt} \right] \tag{25}$$

Then, as $\delta \rightarrow 0$, we obtain as follows:

$$\lim_{\delta \rightarrow 0} \int_{x_1}^{x_2} S(t, x) dx = 0 \tag{26}$$

$$0 = J^-(t, x_1) - S^-(t, x_1) \frac{dx_1(t)}{dt} - \left[J^+(t, x) - S^+(t, x) \frac{dx_s(t)}{dt} \right] \tag{27}$$

From Equation (27), we obtain as follows:

$$\frac{dx_s(t)}{dt} = \frac{J^+(t, x_s) - J^-(t, x_s)}{S^+(t, x_s) - S^-(t, x_s)} \tag{28}$$

The throughput depends on the production density only. Thus, we assume that the production density is constrained by the production volume.

Assumption 2.5.

$$0 \leq S \leq S_{\max} \tag{29}$$

Generally, we obtain as follows.

Definition 2.5.

$$C(t, x^*) \cong \frac{\partial S(t, x^*)}{\partial t} \left(\equiv S(t, x^*) \cdot \frac{dx(t)}{dt} \right) \tag{30}$$

Definition 2.6. *Production flow*

$$J(s) \cong C_{\max} \left[\frac{S_{\max} - S}{S_{\max}} \right] = C_{\max} \left[1 - \frac{S}{S_{\max}} \right] \tag{31}$$

From Equation (31), according to $S \rightarrow S_{\max}$, the production flow $J(s)$ decreases. In other words, the throughput decreases, where C_{\max} represents a maximum value in the given production capacity. Then, we obtain as follows:

$$\frac{dx_s}{dt} \cong \frac{C_{\max} \left\{ S^+ \left[\frac{S_{\max} - S^-}{S_{\max}} \right] - S^- \left[\frac{S_{\max} - S^+}{S_{\max}} \right] \right\}}{S^+ - S^-} = C_{\max} \left(1 - \frac{S^- + S^+}{S_{\max}} \right) \tag{32}$$

Equation (32) represents that the production volume decreases by increasing the throughput with the production capacity constant.

Figure 5 shows the retention situation in which shock waves are generated. Here, shock waves are generated when production stops due to some sudden cause. Production suspension also affects upstream processes. Physically, it corresponds to shock wave propagation. Figure 6 shows the boundary surface of retention and retention period, which we denote as $x \in [0, a(\tau)]$ and $t \in [0, \tau]$, respectively.

2.3. Process retention after stopping production processes. In this Subsection 2.3, we consider process retention after production processes are stopped. Before production stops, we assume that synchronous flow J_0 , i.e., that production is progressing efficiently. Even after production stops, we assume that the subsequent processes propagate similarly as synchronous flow S_0 , as shown in Figure 7.

The time variation is defined as follows.

Definition 2.7. *Stop at any process*

$$\frac{dx_{sl}(t)}{dt} = C_{\max} \left(1 - \frac{S_0 + S_{\max}}{S_{\max}} \right) = -C_{\max} \left(\frac{S_0}{S_{\max}} \right) \tag{33}$$

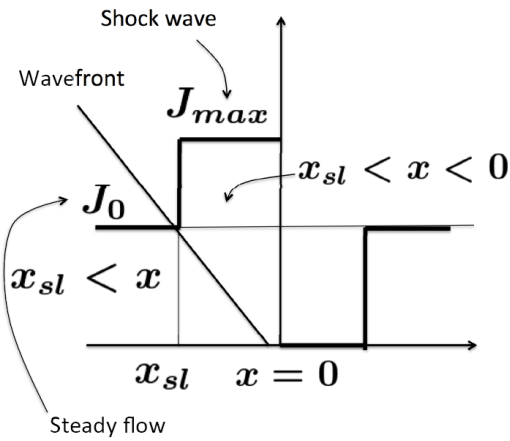


FIGURE 5. Shock wave generation due to suspension of production at $x = 0$

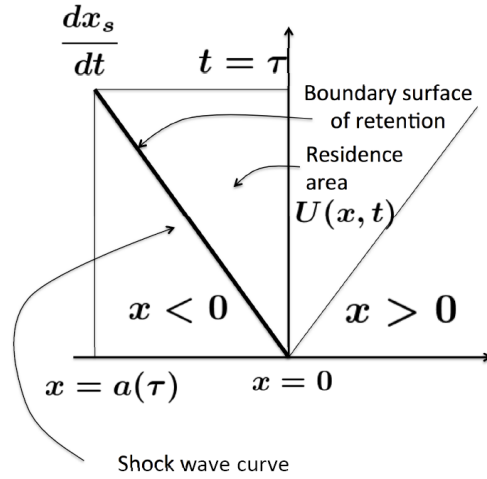


FIGURE 6. Boundary surface of retention

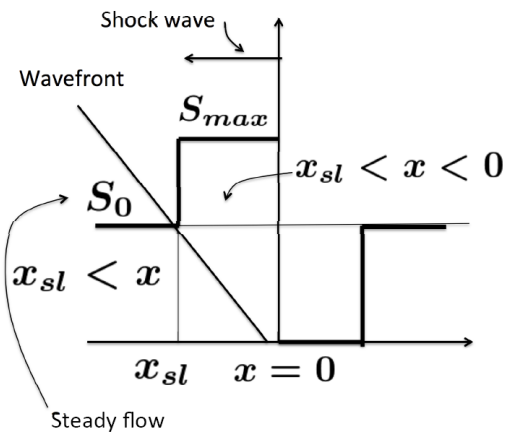


FIGURE 7. Shock wave generation due to suspension of production at $x = 0$

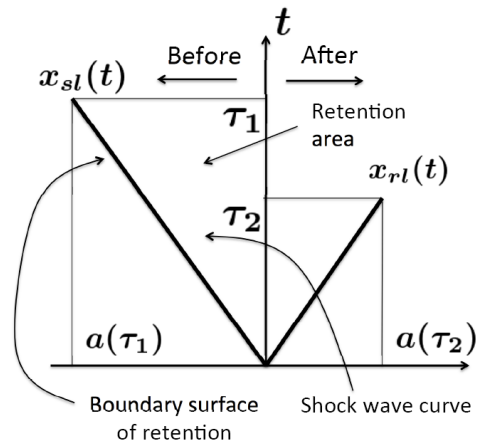


FIGURE 8. Retention after stopping production process

In Figure 7, when $x < x_{sl}$, $S(t, x) = S_0$. When $x_{sl} < x < 0$, $S(t, x) = S_{max}$. From Equation (33), we obtain as follows:

$$x_{sl} = - \int_0^t C_{max} \cdot \frac{S_0}{S_{max}} dt = - \left[\frac{S_0}{S_{max}} \right] C_{max} \cdot t \tag{34}$$

Note that we assume that the retention of the process after the stop in production is retained for at least time τ . Here, let t be time τ from the time production stops to the final process, as depicted in Figure 8. Thus, we obtain as follows:

$$\frac{dx_{sl}(t)}{dt} = \frac{S_0 C(S_0) - 0}{S_0 - 0} = C(S_0) \tag{35}$$

From Equation (35), we obtain as follows:

$$x_{sl}(t) = C(S_0) \cdot t \tag{36}$$

where $C(S_0)$ denotes the synchronous throughput.

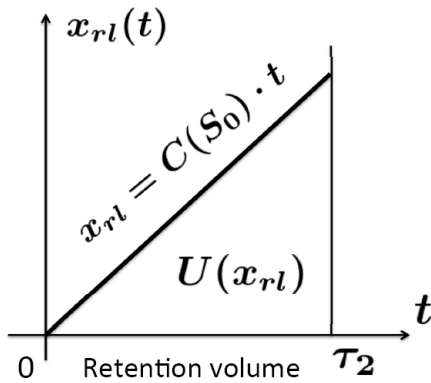


FIGURE 9. Retention volume $U(x_{rl})$

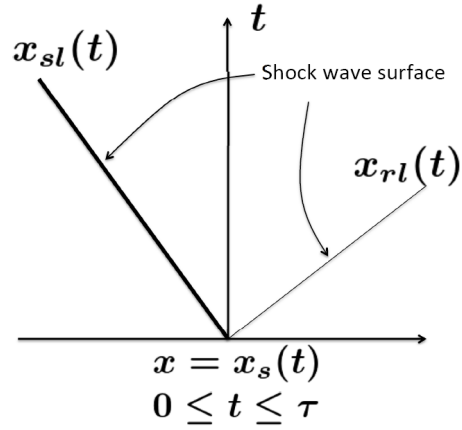


FIGURE 10. Bottle neck point $x = x_s(t)$

In general, depending on the timing of the interruption to the production process, the stop time is different, for example, $\tau_1 \neq \tau_2$ in Figure 8. Here, we can calculate the retention volumes as follows and as shown in Figure 9.

Definition 2.8. Retention volume $U(x_{rl})$

$$U(x_{rl}) = \int_0^{\tau_2} C(S_0) \cdot t dt = \frac{1}{2} C(S_0) \tau_2^2 \tag{37}$$

Similarly, $U(x_{sl})$ can be calculated as follows:

$$U(x_{sl}) = \frac{1}{2} \left[\frac{S_0}{S_{\max}} \right] \cdot C_{\max} \cdot \tau_1^2 \tag{38}$$

From Equations (37) and (38), we obtain the total retention volumes $U(x_s)$ as follows:

$$U(x_s) = \frac{1}{2} \left[\left(\frac{S_0}{S_{\max}} \right) C_{\max} \tau_1^2 + C(S_0) \tau_2^2 \right] \tag{39}$$

2.4. Analysis of bottleneck point $x = x_s(t)$. Figure 10 shows the bottle neck point $x = x_s(t)$. We rewrite the pre-process shock wave as follows:

$$x_{sl}(t) = - \left[\frac{C_{\max} S_0}{S_{\max}} \right] \cdot t \tag{40}$$

We rewrite the post-process shock wave as follows:

$$x_{rl}(t) = - \left[\frac{S_0}{S_{\max}} \right] C_{\max} \cdot t \tag{41}$$

In Figure 11, the production density flow denotes the production propagation equations as follows:

$$\frac{\partial S}{\partial t} + v \frac{\partial S}{\partial x} = 0 \tag{42}$$

where v satisfies the following equation.

$$v = \frac{\partial J}{\partial S} \tag{43}$$

$x = 0$ denotes the bottle neck stop point in Figure 12.

$$S(x, 0) = S_{\max}; \quad x < 0 \tag{44}$$

$$S(x, 0) = 0; x < 0 \tag{45}$$

Equation (44) denotes the post-processes retention and Equation (45) denotes the pre-processes empty. The characteristic curve is derived at $t = 0$ as follows:

$$x = C_{\max} \cdot t + x_0 \tag{46}$$

where $x = x_0 > 0$.

Similarly, we obtain as follows:

$$x = -C_{\max} \cdot t + x_0 \tag{47}$$

where $x = x_0 < 0$.

$S = 0$ and $S = S_{\max}$ are obtained along this straight line, which are Equation (46) or Equation (47).

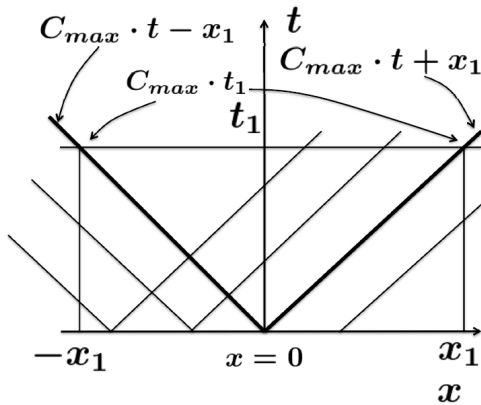


FIGURE 11. Characteristic curve of shock wave

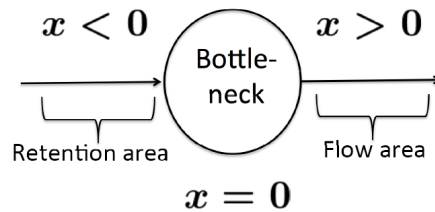


FIGURE 12. Bottle neck point $x = x_s(t)$

According to Equation (31), we obtain as follows:

$$J(s) = C_{\max} \left[1 - \frac{S}{S_{\max}} \right] \tag{48}$$

where x_1 satisfies $-C_{\max} \cdot t < x_1 < C_{\max} \cdot t$.

Moreover, the characteristic curve passing through point (x_1, t) and point $(0, 0)$ is derived as follows:

$$x = \frac{\partial J}{\partial S} \cdot t \tag{49}$$

From Equation (49), we obtain as follows:

$$\frac{x}{t} = \frac{\partial J}{\partial S} = C(S) + SC'(S) = C_{\max} \left[1 - \frac{2S}{S_{\max}} \right] \tag{50}$$

From Equation (50), S is obtained as follows:

$$S(t, x) = \frac{S_{\max}}{2} \left(1 - \frac{x}{C_{\max} \cdot t} \right) \tag{51}$$

where x represents the position of the production flow.

At this time, x is constrained by the following equation.

$$-C_{\max} \cdot t < x < C_{\max} \cdot t \tag{52}$$

3. Numerical Result.

3.1. Numerical simulation. Equation (52) represents the production density with respect to (x, t) . More specifically, Equations (51) and (52) show the change in production density from when production stopped to when it started back up again, i.e., the propagation of shock waves is a phenomenon of queuing time constraints due to retention. Please refer to Appendix A. The place marked with a circle is the place that shows retention.

With respect to Figure 13, the throughput represents Test run 3 > Test run 2 > Test run 1. C_{max} sets S3(199min)/work number of people(9) = 22.1 of Test run 1, sets S2(196min)/work number of people(9) \simeq 20.1 and sets S4(180min)/work number of people(9) = 20. S_{max} is the production density, which is calculated from the throughput ratio of Test runs 1-3 in Appendix A. However, it is the value when we set 5 to Test run 1. S_{max} is calculated from the ratio of Test run 2/Test run 3 to C_{max} of Test run 1. In actual data, the production number of Test run 1-3 is 4.4 units/month, 5.5 units/month and 5.7 units/month, respectively.

3.2. Dynamic simulation of production processes. We attempted to perform a dynamic simulation of the production process by utilizing the simulation system that NTT DATA Mathematical Systems Inc. (www.msi.co.jp) has developed. With respect to the meaning of the individual parts in Figure 15, we conducted a simulation of the following

TABLE 1. Parameter setting of Figure 13

| Figure 13 | Test run 1 | Test run 2 | Test run 3 |
|-----------|------------|------------|------------|
| S_{max} | 5 | 5.1 | 5.5 |
| C_{max} | 22.1 | 20.1 | 20 |

TABLE 2. Parameter setting of Figure 14

| Figure 14 | Test run 1 | Test run 2 | Test run 3 |
|-----------|------------|------------|------------|
| S_{max} | 5 | 5.1 | 5.5 |
| C_{max} | 22.1 | 20.1 | 20 |

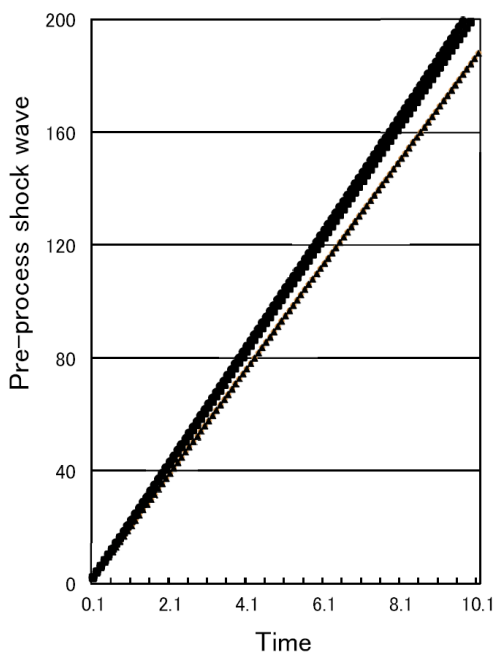


FIGURE 13. Pre-process shock wave at retention surface

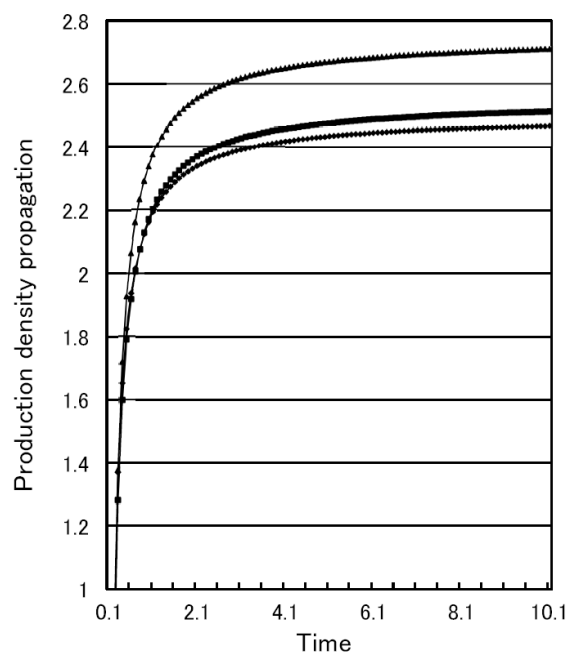


FIGURE 14. Production density propagation from production stop to start

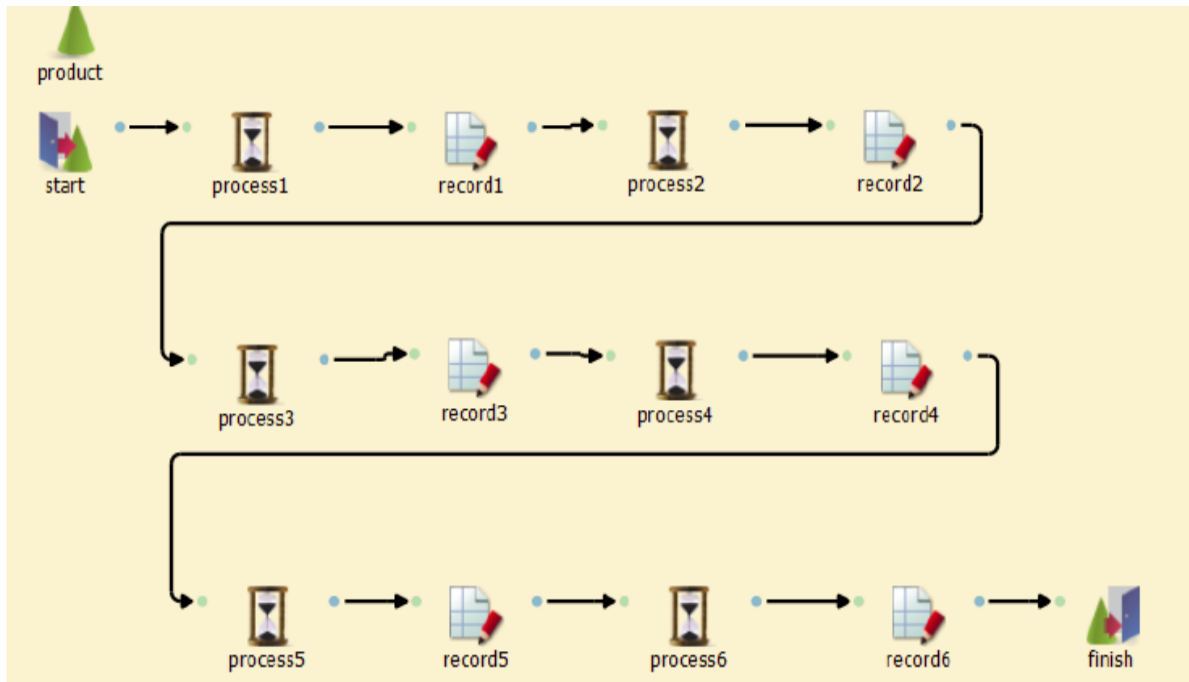


FIGURE 15. Simulation model of production flow system

TABLE 3. Working data for six production asynchronous processes

| Process No. | No.1 | No.2 | No.3 | No.4 | No.5 | No.6 |
|-------------|------|------|------|------|------|------|
| Average | 20 | 22 | 25 | 22 | 25 | 21 |
| STD | 2.1 | 2.5 | 1.6 | 1.9 | 2.0 | 1.9 |
| W.E 1 | 0.83 | 1.0 | 0.66 | 0.76 | 0.88 | 0.91 |
| W.E 2 | 1.27 | 1.26 | 1.21 | 1.31 | 1.17 | 1.20 |
| W.E 3 | 0.96 | 1.11 | 1.01 | 1.12 | 0.88 | 0.89 |
| W.E 4 | 0.92 | 0.96 | 1.06 | 0.98 | 0.91 | 0.9 |
| W.E 5 | 1.2 | 1.03 | 1.07 | 0.89 | 1.03 | 1.1 |
| W.E 6 | 1.09 | 1.1 | 1.2 | 0.98 | 1.13 | 0.89 |

TABLE 4. Working data for six production synchronous processes

| Process No. | No.1 | No.2 | No.3 | No.4 | No.5 | No.6 |
|-------------|------|------|------|------|------|------|
| Average | 20 | 20 | 20 | 20 | 20 | 20 |
| STD | 1.1 | 1.5 | 1.2 | 1.4 | 1.0 | 1.4 |
| W.E 1 | 1.0 | 1.0 | 1.0 | 1.0 | 1.0 | 1.0 |
| W.E 2 | 1.0 | 1.0 | 1.2 | 1.3 | 1.1 | 1.2 |
| W.E 3 | 1.7 | 1.1 | 1.0 | 1.1 | 1.0 | 1.0 |
| W.E 4 | 1.0 | 1.0 | 1.0 | 1.0 | 1.0 | 1.0 |
| W.E 5 | 1.0 | 1.0 | 1.0 | 1.0 | 1.0 | 1.0 |
| W.E 6 | 1.0 | 1.3 | 1.2 | 1.0 | 1.1 | 1.0 |

procedure. When the simulation began, it generated one of the products on a “start” part to “finish”.

- In each process, including the six workers in parallel, the slowest worker waited till the work was completed.
- When the work of each process was completed, it moved to the next process.
- Simultaneously as each process was completed, it recorded the working time of each process.

With respect to Table 3 and Table 4,

- Process No. indicates each process (1-6).
- Average indicates the average time.
- STD indicates the standard deviation of process time (sec).
- Worker efficiency (WE) indicates the efficiency of six workers.

“record” calculates the worker’s operating time, which is obtained by multiplying the specified WE data for the log-normally distributed random numbers in Table 3.

Figure 16 shows the operating time of processes 1-6 (record1-record6). As the working time of the synchronous process is less volatile, the work efficiency became higher than the asynchronous process. In Figure 16, the total working time of asynchronous and synchronous processes are 1241.7(sec) and 586.4(sec) respectively. The synchronous process shows much better production efficiency than the asynchronous process.

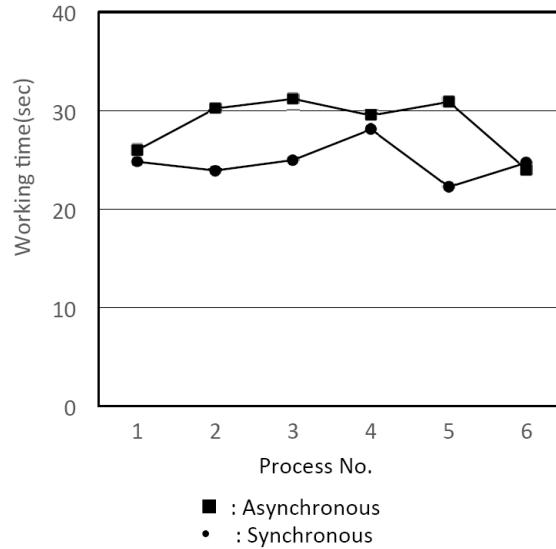


FIGURE 16. Working time for process number one through six

4. Conclusions. In this paper, we mathematically analyzed the phenomena that occur before and after an interruption to production processes. We also analyzed the resulting shock wave propagation of production density flows using Burgers’ equation. Through our work, given that we were able to mathematically analyze the behavior before and after an interruption to production, we can better predict future production problems and how best to react to them. Previous studies utilizing the Burgers equation for the mathematical retention analysis for the production process have not been reported yet. We think that it will become a trigger to further improve productivity by analyzing the retention of production process. In our future work, we plan to focus on shock wave analysis for mathematical models that consider a stochastic model.

REFERENCES

[1] K. Nishioka, Y. Mizutani, H. Ueno et al., Toward the integrated optimization of steel plate production process – A proposal for production control by multi-scale hierarchical modeling –, *Synthesiology*, vol.5, no.2, pp.98-112, 2012.

[2] S. D. Treville, R. D. Shapiro and A. Hameri, From supply chain to demand chain: The role of lead time reduction in improving demand chain performance, *Journal of Operations Management*, vol.21, no.6, pp.613-627, 1995.

[3] I. P. Tasiopoulos and B. G. Kingsman, Lead time management, *European Journal of Operational Research*, vol.14, no.4, pp.351-358, 1983.

[4] S. Hiiragi, *The Significance of Shortening Lead Time from a Business Perspective*, <http://merc.e.u-tokyo.ac.jp/mmrc/dp/index.html>, MMRC, University of Tokyo, 2012 (in Japanese).

[5] N. Ueno, M. Kawasaki, H. Okuhira and T. Kataoka, Mass customization production planning system for multi-process, *Journal of the Faculty of Management and Information Systems, Prefectural University of Hiroshima*, no.1, pp.183-192, 2009 (in Japanese).

- [6] H. L. Lee, V. Padmanabhan and S. Whang, The bullwhip effect in supply chains, *Sloan Management Review*, pp.93-102, 1997.
- [7] H. Kondo and K. Nisinari, Modeling stock congestion in production management, *Reports of RIAM Symposium, Mathematics and Physics in Nonlinear Waves*, pp.146-149, 2008 (in Japanese).
- [8] S. J. Baderstone and V. J. Mabin, A review Goldratt's theory of constraints (TOC) – Lessons from the international literature, *Operations Research Society of New Zealand the 33rd Annual Conference*, University of Auckland, New Zealand, 1998.
- [9] K. Shirai and Y. Amano, Production density diffusion equation and production, *IEEJ Trans. Electronics, Information and Systems*, vol.132-C, no.6, pp.983-990, 2012.
- [10] K. Shirai and Y. Amano, A study on mathematical analysis of manufacturing lead time – Application for deadline scheduling in manufacturing system –, *IEEJ Trans. Electronics, Information and Systems*, vol.132-C, no.12, pp.1973-1981, 2012.
- [11] K. Shirai, Y. Amano and S. Omatu, Improving throughput by considering the production process, *International Journal of Innovative Computing, Information and Control*, vol.9, no.12, pp.4917-4930, 2013.
- [12] K. Shirai, Y. Amano and S. Omatu, Propagation of working-time delay in production, *International Journal of Innovative Computing, Information and Control*, vol.10, no.1, pp.169-182, 2014.
- [13] K. Shirai and Y. Amano, Throughput improvement strategy for nonlinear characteristics in the production processes, *International Journal of Innovative Computing, Information and Control*, vol.10, no.6, pp.1983-1997, 2014.
- [14] K. Shirai, Y. Amano and S. Omatu, Process throughput analysis for manufacturing process under incomplete information based on physical approach, *International Journal of Innovative Computing, Information and Control*, vol.9, no.11, pp.4431-4445, 2013.
- [15] K. Shirai and Y. Amano, Production throughput evaluation using the Vasicek model, *International Journal of Innovative Computing, Information and Control*, vol.11, no.1, pp.1-17, 2015.
- [16] K. Shirai and Y. Amano, On-off intermittency management for production process improvement, *International Journal of Innovative Computing, Information and Control*, vol.11, no.3, pp.815-831, 2015.
- [17] H. Tasaki, *Thermodynamics – A Contemporary Perspective (New Physics Series)*, Baifukan, Co., LTD, pp.20-80, 2000.
- [18] K. Shirai and Y. Amano, Synchronization analysis of a production process utilizing stochastic resonance, *International Journal of Innovative Computing, Information and Control*, vol.12, no.3, pp.899-914, 2016.
- [19] K. Kamamura, H. Oh et al., *Higher-Order Approximation of the Burgers Equation*, Research Institute for Mathematical Sciences, Kyoto University, vol.993, pp.35-45, 1997.
- [20] K. Shirai and Y. Amano, Synchronization analysis of the production process utilizing the phase-field model, *International Journal of Innovative Computing, Information and Control*, vol.12, no.5, pp.1597-1613, 2016.
- [21] K. Shirai and Y. Amano, Analysis of fluctuations in production processes using Burgers equation, *International Journal of Innovative Computing, Information and Control*, vol.12, no.6, pp.1615-1628, 2016.
- [22] S. Urata and S. Watanabe, The experiments of burgers system, *Publications of the Research Institute for Mathematical Sciences*, vol.1271, pp.226-232, 2002.
- [23] K. Shirai and Y. Amano, Analysis of production processes using a lead-time function, *International Journal of Innovative Computing, Information and Control*, vol.12, no.1, pp.125-138, 2016.
- [24] K. Shirai and Y. Amano, Nonlinear characteristics of the rate of return in the production process, *International Journal of Innovative Computing, Information and Control*, vol.10, no.2, pp.601-618, 2014.
- [25] T. Takagi and A. Yamanaka, *Phase Field Method – Material Organization Design by Numerical Simulation –*, Yokendo Co. LTD, 2012.
- [26] K. Shirai and Y. Amano, Validity of production flow determined by the phase difference in the gradient system of an autonomous decentralized system, *International Journal of Innovative Computing, Information and Control*, vol.10, no.5, pp.1727-1745, 2014.
- [27] K. Shirai, Y. Amano, S. Omatu and E. Chikayama, Power-law distribution of rate-of-return deviation and evaluation of cash flow in a control equipment manufacturing company, *International Journal of Innovative Computing, Information and Control*, vol.9, no.3, pp.1095-1112, 2013.
- [28] T. Tatumi, *Fluid Dynamics (New Physics Series)*, Baifukan, Co., LTD, 1995.
- [29] K. Kitahara, *Statistical Mechanics of Non-Equilibrium System*, Iwanami Shoten Co. LTD, 2000.

Appendix A. Analysis of the Testrun Results.

- (Testrun1): Because the throughput of each process (S1-S6) is asynchronous, the overall process throughput is asynchronous. In Table 6, we list the manufacturing time (min) of each process. In Table 7, we list the volatility in each process performed by the workers. Finally, Table 6 lists the target times. The theoretical throughput is obtained as $3 \times 199 + 2 \times 15 = 627$ (min). In addition, the total working time in stage S3 is 199 (min), which causes a bottleneck. In Figure 17, we plot the measurement data listed in Table 6, which represents the total working time of each worker (K1-K9). In Figure 18, we plot the data contained in Table 6, which represents the volatility of the working times.
- (Testrun2): Set to synchronously process the throughput. The target time listed in Table 8 is 500 (min), and the theoretical throughput (not including the synchronization idle time) is 400 (min). Table 9 presents the volatility of each working process (S1-S6) for each worker (K1-K9).
- (Testrun3): Introducing a preprocess stage. The process throughput is performed synchronously with the reclassification of the process. As shown in Table 10, the theoretical throughput (not including the synchronization idle time) is 400 (min). Table 11 presents the volatility of each working process (S1-S6) for each worker (K1-K9). On the basis of these results, the idle time must be set to 100 (min). Moreover, the theoretical target throughput (T'_s) can be obtained using the “Synchronization with preprocess” method. This goal is as follows:

$$\begin{aligned}
 T_s &\sim 20 \times 6 \text{ (First cycle)} + 17 \times 6 \text{ (Second cycle)} \\
 &\quad + 20 \times 6 \text{ (Third cycle)} + 20 \text{ (Previous process)} + 8 \text{ (Idle - time)} \\
 &\sim 370 \text{ (min)}
 \end{aligned}
 \tag{53}$$

The full synchronous throughput in one stage (20 min) is

$$T'_s = 3 \times 120 + 40 = 400 \text{ (min)}
 \tag{54}$$

Using the “Synchronization with preprocess” method, the throughput is reduced by approximately 10%. Therefore, we showed that our proposed “Synchronization with preprocess” method is realistic and can be applied in flow production systems. Below, we represent for a description of the “Synchronization with preprocess”.

In Table 10, the working times of the workers K4, K7 show shorter than others. However, the working time shows around target time. Next, we manufactured one piece of equipment in three cycles. To maintain a throughput of six units/day, the production throughput must be as follows:

$$\frac{(60 \times 8 - 28)}{3} \times \frac{1}{6} \simeq 25 \text{ (min)}
 \tag{55}$$

where the throughput of the preprocess is set to 20 (min). In Equation (55), the value 28 represents the throughput of the preprocess plus the idle time for synchronization. Similarly, the number of processes is 8 and the total number of processes is 9 (8 plus the preprocess). The value of 60 is obtained as 20 (min) \times 3 (cycles).

In Table 5, Test-run3 indicates a best value for the throughput in the three types of theoretical working time. Test-run2 is ideal production method. However, because it is difficult for talented worker, Test-run3 is a realistic method.

The results are as follows. Here, the trend coefficient, which is the actual number of pieces of equipment/the target number of equipment, represents a factor that indicates the degree of the number of pieces of manufacturing equipment.

Test-run1: $4.4 \text{ (pieces of equipment)} / 6 \text{ (pieces of equipment)} = 0.73,$

TABLE 5. Correspondence between the table labels and the Test-run number

| | Table number | Production process | Working time | Volatility |
|-----------|--------------|--|--------------|------------|
| Test-run1 | Table 6 | Asynchronous process | 627 (min) | 0.29 |
| Test-run2 | Table 8 | Synchronous process | 500 (min) | 0.06 |
| Test-run3 | Table 10 | “Synchronization with preprocess” method | 470 (min) | 0.03 |

TABLE 6. Total manufacturing time at each stages for each worker

| | WS | S1 | S2 | S3 | S4 | S5 | S6 |
|-----------|-----|-----|-----|-----|-----|-----|-----|
| K1 | 15 | 20 | 20 | 25 | 20 | 20 | 20 |
| K2 | 20 | 22 | 21 | 22 | 21 | 19 | 20 |
| K3 | 10 | 20 | 26 | 25 | 22 | 22 | 26 |
| K4 | 20 | 17 | 15 | 19 | 18 | 16 | 18 |
| K5 | 15 | 15 | 20 | 18 | 16 | 15 | 15 |
| K6 | 15 | 15 | 15 | 15 | 15 | 15 | 15 |
| K7 | 15 | 20 | 20 | 30 | 20 | 21 | 20 |
| K8 | 20 | 29 | 33 | 30 | 29 | 32 | 33 |
| K9 | 15 | 14 | 14 | 15 | 14 | 14 | 14 |
| Total | 145 | 172 | 184 | 199 | 175 | 174 | 181 |
| Deviation | | 27 | 39 | 54 | 30 | 29 | 36 |

TABLE 7. Volatility of Table 6

| | | | | | | |
|----|------|------|------|------|------|------|
| K1 | 1.67 | 1.67 | 3.33 | 1.67 | 1.67 | 1.67 |
| K2 | 2.33 | 2 | 2.33 | 2 | 1.33 | 1.67 |
| K3 | 1.67 | 3.67 | 3.33 | 2.33 | 2.33 | 3.67 |
| K4 | 0.67 | 0 | 1.33 | 1 | 0.33 | 1 |
| K5 | 0 | 1.67 | 1 | 0.33 | 0 | 0 |
| K6 | 0 | 0 | 0 | 0 | 0 | 0 |
| K7 | 1.67 | 1.67 | 5 | 1.67 | 2 | 1.67 |
| K8 | 4.67 | 6 | 5 | 4.67 | 5.67 | 6 |
| K9 | 0.33 | 0.33 | 0 | 0.33 | 0.33 | 0.33 |

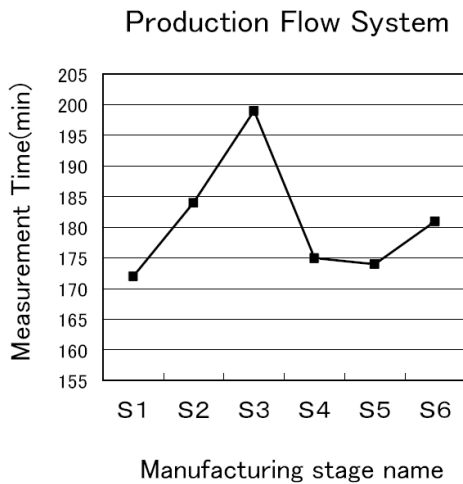


FIGURE 17. Total work time for each stage (S1-S6) in Table 6

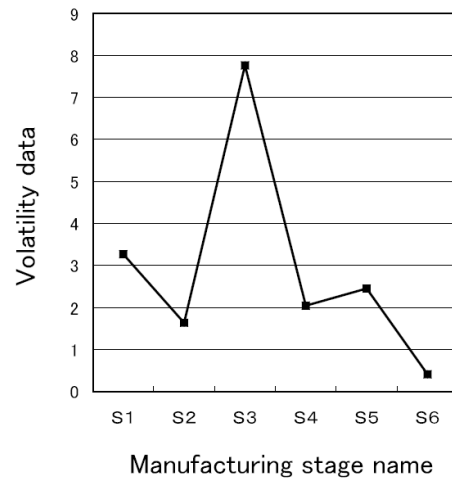


FIGURE 18. Volatility data for each stage (S1-S6) in Table 6

Test-run2: $5.5 \text{ (pieces of equipment)} / 6 \text{ (pieces of equipment)} = 0.92$,

Test-run3: $5.7 \text{ (pieces of equipment)} / 6 \text{ (pieces of equipment)} = 0.95$.

Volatility data represent the average value of each Test-run.

TABLE 8. Total manufacturing time at each stage for each worker

| | WS | S1 | S2 | S3 | S4 | S5 | S6 |
|-----------|-----|-----|-----|-----|-----|-----|-----|
| K1 | 20 | 20 | 24 | 20 | 20 | 20 | 20 |
| K2 | 20 | 20 | 20 | 20 | 20 | 22 | 20 |
| K3 | 20 | 20 | 20 | 20 | 20 | 20 | 20 |
| K4 | 20 | 25 | 25 | 20 | 20 | 20 | 20 |
| K5 | 20 | 20 | 20 | 20 | 20 | 20 | 20 |
| K6 | 20 | 20 | 20 | 20 | 20 | 20 | 20 |
| K7 | 20 | 20 | 20 | 20 | 20 | 20 | 20 |
| K8 | 20 | 27 | 27 | 22 | 23 | 20 | 20 |
| K9 | 20 | 20 | 20 | 20 | 20 | 20 | 20 |
| Total | 180 | 192 | 196 | 182 | 183 | 182 | 180 |
| Deviation | | 12 | 16 | 2 | 3 | 2 | 0 |

TABLE 9. Volatility of Table 8

| | | | | | | |
|----|------|------|------|---|------|---|
| K1 | 0 | 1.33 | 0 | 0 | 0 | 0 |
| K2 | 0 | 0 | 0 | 0 | 0.67 | 0 |
| K3 | 0 | 0 | 0 | 0 | 0 | 0 |
| K4 | 1.67 | 1.67 | 0 | 0 | 0 | 0 |
| K5 | 0 | 0 | 0 | 0 | 0 | 0 |
| K6 | 0 | 0 | 0 | 0 | 0 | 0 |
| K7 | 0 | 0 | 0 | 0 | 0 | 0 |
| K8 | 2.33 | 2.33 | 0.67 | 1 | 0 | 0 |
| K9 | 0 | 0 | 0 | 0 | 0 | 0 |

TABLE 10. Total manufacturing time at each stage for each worker

| | WS | S1 | S2 | S3 | S4 | S5 | S6 |
|-----------|-----|-----|-----|-----|-----|-----|-----|
| K1 | 20 | 18 | 19 | 18 | 20 | 20 | 20 |
| K2 | 20 | 18 | 18 | 18 | 20 | 20 | 20 |
| K3 | 20 | 21 | 21 | 21 | 20 | 20 | 20 |
| K4 | 20 | 13 | 11 | 11 | 20 | 20 | 20 |
| K5 | 20 | 16 | 16 | 17 | 20 | 20 | 20 |
| K6 | 20 | 18 | 18 | 18 | 20 | 20 | 20 |
| K7 | 20 | 14 | 14 | 13 | 20 | 20 | 20 |
| K8 | 20 | 22 | 22 | 20 | 20 | 20 | 20 |
| K9 | 20 | 25 | 25 | 25 | 20 | 20 | 20 |
| Total | 180 | 165 | 164 | 161 | 180 | 180 | 180 |
| Deviation | | -15 | -16 | -19 | 0 | 0 | 0 |

TABLE 11. Volatility of Table 10

| | | | | | | |
|----|------|------|------|---|---|---|
| K1 | 0.67 | 0.33 | 0.67 | 0 | 0 | 0 |
| K2 | 0.67 | 0.67 | 0.67 | 0 | 0 | 0 |
| K3 | 0.33 | 0.33 | 0.33 | 0 | 0 | 0 |
| K4 | 2.3 | 3 | 3 | 0 | 0 | 0 |
| K5 | 1.3 | 1.3 | 1 | 0 | 0 | 0 |
| K6 | 0.67 | 0.67 | 0.67 | 0 | 0 | 0 |
| K7 | 2 | 2 | 2.3 | 0 | 0 | 0 |
| K8 | 0.67 | 0.67 | 0 | 0 | 0 | 0 |
| K9 | 1.67 | 1.67 | 1.67 | 0 | 0 | 0 |